Slip Effects on the Peristaltic Flow of a Carreau Fluid in a Planar Channel under the Effect of a Magnetic Field

B. Jyothi[1], Aws Safaa Mahdi[2], B. Satyanarayana[3]

[1]Department of Mathematics, DNR College, Bhimavaram, A.P, India

[2, 3]Department of Mathematics, Acharya Nagarjuna University, Nagarjuna Nagar-522 510, India

Abstract: *In this paper, we studied the effects slip on the peristaltic flow of a Carreau fluid in a two dimensional channel under the assumptions of low Reynolds number and long wavelength. The flow is investigated in a wave frame of reference moving with velocity of the wave. The perturbation series in the Weissenberg number ($We < 1$) was used to obtain explicit forms for velocity field, pressure gradient per one wavelength. The effects of various pertinent parameters on the pressure gradient and pumping characteristics are discussed through graphs in detail.*

Keywords: Weissenberg number, Hartmann number; Peristaltic flow and, Carreau fluid

1. Introduction

Many authors have studied the analysis of the mechanisms for peristaltic transport of non-Newtonian fluids. Srivastava and Srivastava (1985) have investigated the effects of power- law fluid in uniform and non - uniform tubes under zero Reynolds number and long wavelength approximations. Siddiqui and Schwarz (1994) have investigated the peristaltic flow of a second order fluid in a tube and have used a perturbation method to second order in dimensionless wave number. The Carreau fluid model is a four parameter model. El-Misery et al. (1996) have investigated the peristaltic transport of carreau fluid through a uniform channel, under zero Reynolds number and long wave length approximations. Elshehawey et al. (1998) have investigated the peristaltic transport of Carreau fluid through a non uniform channel, under zero Reynolds number and long wavelength approximations. Abd El Hakeem and El-Misiery (2002) have investigated the peristaltic pumping of Carreau fluid in the presence of an endoscope. Separation in the flow through peristaltic motion of a Carreau fluid in uniform tube is discussed by Abd El Hakeem et al. (2004). Ali and Hayat (2007) have studied the peristaltic flow of a Carreau fluid in an asymmetric channel.

Fluid dynamics of magneto hydrodynamic (MHD) fluid has from historic times been the object of scientific and engineering research. Also, it is known that most of the physiological fluids are non-Newtonian fluid. Specifically, the non-Newtonian fluids in the presence of a magnetic field are very useful in magneto-therapy. The controlled application of low intensity and frequency pulsing magnetic fields modify the cell and tissue behavior. Moreover, the non-invasive radiological test that uses a magnetic field (not radiation) to evaluate organs in abdomen prior to surgery in the small intestine (but not always). Hence magnetically susceptible of chyme can be satisfied from the heat generated by magnetic field or the ions contained in the chyme. The peristaltic flows of magneto hydrodynamic (MHD) fluid have been studied by stud et al. (1977), Srivastava and Agrawal(1980), Agrawal and Anwaruddin (1984), Mekheimer (2004), Shahed and Horoun (2005), Siddiqui et al. (2004) and Hayat et al. (2005).

All the above investigations on peristaltic transport have been made taking into account the classical no- slip boundary conditions. However, in several applications, the flow pattern corresponds to slip flow and the fluid presents a loss of adhesion at the wetted wall making the fluid slide along the wall. Flows with slip would be use full for problems in engineering, for example flows through pipe in which chemical reactions occur at the walls, two phase flow in porous slider bearings. The initial work on slip boundary conditions were done by Beaver and Joseph. The theoretical justification of the boundary conditions of Beaver and Joseph was given by Saffman and proposed improved boundary conditions. El Sehaway et al. (2006) have discussed the effect of slip on the peristaltic motion of a Maxwell fluid in a channel. The effects of slip and non-Newtonian parameters on the peristaltic flow of a third grade fluid in a circular cylindrical tube were investigated by Ali et al. (2009). Chaube et al. (2010) have studied the slip effects on the peristaltic flow of a micropolar fluid in a channel. Effects of slip and induced magnetic field on the peristaltic flow of pseudoplastic fluid were analyzed by Noreen et al. (2011). Recently, Subba Reddy et al. (2012) have investigated the slip effects on the peristaltic transport of a Jeffrey fluid through a porous medium in an asymmetric channel under the effect magnetic field.

In view of these, we studied the effects slip on the peristaltic flow of a Carreau fluid in a two dimensional channel under the assumptions of low Reynolds number and long wavelength. The flow is investigated in a wave frame of reference moving with velocity of the wave. The perturbation series in the Weissenberg number ($We < 1$) was used to obtain explicit forms for velocity field, pressure gradient per one wavelength. The effects of various pertinent parameters on the pressure gradient and pumping characteristics are discussed through graphs in detail.

2. Mathematical Formulation

We consider the two-dimensional flow of an incompressible Carreau fluid in a two dimensional channel with flexible walls. It is assumed that the progressive sinusoidal waves propagate along the walls of the channel. The fluid subjected to a constant transverse magnetic field. Induced magnetic field, external electric field, electric field due to polarization of charges, heat due to viscous and joule dissipation are neglected. The equation of the channel wall is given by

$$Y = H(X,t) = a + b\cos\frac{2\pi}{\lambda}(X - ct), \quad (2.1)$$

where b, λ, c and a are amplitude, wave length, phase speed of the wave, mean-half width of the channel respectively, t is the time and (X, Y) are the Cartesian co-ordinates. Fig.1 represents the physical model of the channel.
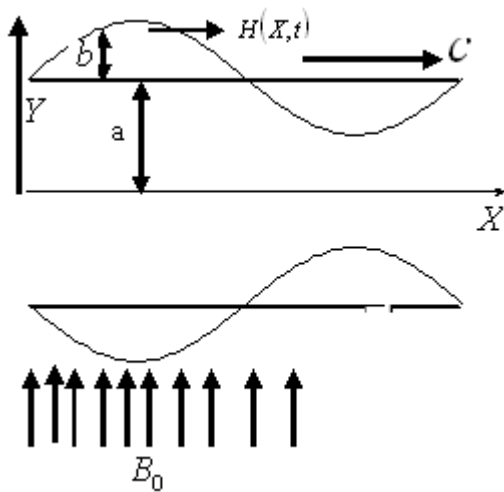

Figure 1: The physical model

We introduce a wave frame of reference (x, y) moving with the velocity c in which the motion becomes independent of time when the channel length is an integral multiple of the wave length and the pressure difference at the ends of the channel is a constant (Shapiro et al., 1969). The transformation from the fixed frame of reference (X, Y) to the wave frame of reference (x, y) is given by

$$x = X - ct, \quad y = Y, \quad u = U - c,$$
$$v = V, \quad p(x) = P(X,t) \quad (2.2)$$

where (u, v) and (U, V) are the velocity components, p and P are pressures in the wave and fixed frames of reference respectively.

The constitute equation for a Carreau fluid (given in Bird et al., 1977) is

$$\tau = -\left[\eta_\infty + (\eta_0 - \eta_\infty)\left(1 + (\Gamma\dot{\gamma})^2\right)^{\frac{n-1}{2}}\right]\dot{\gamma} \quad (2.3)$$

where τ is the extra stress tensor, η_∞ is the infinite shear rate viscosity, η_0 is the zero shear rate viscosity, Γ is the

time constant, n is the dimensionless power-law index and $\dot{\gamma}$ is defined as

$$\dot{\gamma} = \sqrt{\frac{1}{2}\sum_i\sum_j\dot{\gamma}_{ij}\dot{\gamma}_{ji}} = \sqrt{\frac{1}{2}\pi} \quad (2.4)$$

here π is the second invariant of strain-rate tensor. We consider in the constitutive Eq. (2.3) the case for which $\eta_\infty = 0$ and so we can write

$$\tau = -\eta_0\left(1 + (\Gamma\dot{\gamma})^2\right)^{\frac{n-1}{2}}\dot{\gamma}. \quad (2.5)$$

The above model reduces to Newtonian model for $n = 1$ (or) $\Gamma = 0$

The equations governing the flow in the wave frame of reference are

$$\frac{\partial u}{\partial x} + \frac{\partial v}{\partial y} = 0 \quad (2.6)$$

$$\rho\left(u\frac{\partial u}{\partial x} + v\frac{\partial u}{\partial y}\right) = -\frac{\partial p}{\partial x} - \frac{\partial \tau_{xx}}{\partial x} - \frac{\partial \tau_{yx}}{\partial y} - \sigma B_0^2(u+1) \quad (2.7)$$

$$\rho\left(u\frac{\partial v}{\partial x} + v\frac{\partial v}{\partial y}\right) = -\frac{\partial p}{\partial y} - \frac{\partial \tau_{xy}}{\partial x} - \frac{\partial \tau_{yy}}{\partial y} \quad (2.8)$$

where ρ is the density, σ is the electrical conductivity and B_0 is constant transverse magnetic field.

Introducing the non-dimensional variable defined by

$$\bar{x} = \frac{x}{\lambda}, \quad \bar{y} = \frac{y}{a}, \quad \bar{u} = \frac{u}{c}, \quad \bar{v} = \frac{v}{c\delta}, \quad \delta = \frac{a}{\lambda},$$

$$\bar{p} = \frac{pa^2}{\eta_0 c\lambda}, \quad h = \frac{H}{a}, \bar{t} = \frac{ct}{\lambda}, \quad \bar{\tau}_{xx} = \frac{\lambda}{\eta_0 c}\tau_{xx},$$

$$\bar{\tau}_{xy} = \frac{a}{\eta_0 c}\tau_{xy}, \quad \bar{\tau}_{yy} = \frac{a}{\eta_0 c}\tau_{yy}, \quad \text{Re} = \frac{\rho ac}{\eta_0},$$

$$We = \frac{\Gamma c}{a}, \quad \bar{\dot{\gamma}} = \frac{\dot{\gamma}a}{c}, \quad \bar{q} = \frac{q}{ac}, \quad (2.9)$$

where Re is the Reynolds number and δ is the wave number, into the equations (2.6) – (2.8) (dropping bars), we get

$$\frac{\partial u}{\partial x} + \frac{\partial v}{\partial y} = 0 \quad (2.10)$$

$$\text{Re}\,\delta\left(u\frac{\partial u}{\partial x} + v\frac{\partial u}{\partial y}\right)$$
$$= -\frac{\partial p}{\partial x} - \frac{\delta^2}{\varepsilon}\frac{\partial \tau_{xx}}{\partial x} - \frac{1}{\varepsilon}\frac{\partial \tau_{yx}}{\partial y} - \left(\frac{1}{Da} + M^2\right)(u+1) \quad (2.11)$$

$$\text{Re}\,\delta^3\left(u\frac{\partial v}{\partial x} + v\frac{\partial v}{\partial y}\right).$$
$$= -\frac{\partial p}{\partial y} - \frac{\delta^2}{\varepsilon}\frac{\partial \tau_{xy}}{\partial x} - \delta\frac{\partial \tau_{yy}}{\partial y} - \frac{\delta^2}{Da}v \quad (2.12)$$

Where

Paper ID: ART20171038

355

$$\tau_{xx} = -2\left[1+\left(\frac{n-1}{2}\right)We^2\dot\gamma^2\right]\frac{\partial u}{\partial x},$$

$$\tau_{xy} = -\left[1+\left(\frac{n-1}{2}\right)We^2\dot\gamma^2\right]\left(\frac{\partial u}{\partial y}+\delta^2\frac{\partial v}{\partial x}\right),$$

$$\tau_{yy} = -2\delta\left[1+\left(\frac{n-1}{2}\right)We^2\dot\gamma^2\right]\frac{\partial v}{\partial y},$$

$$\dot\gamma = \left[2\delta^2\left(\frac{\partial u}{\partial x}\right)^2+\left(\frac{\partial u}{\partial y}-\delta^2\frac{\partial v}{\partial x}\right)+2\delta^2\left(\frac{\partial v}{\partial y}\right)^2\right]^{\frac{1}{2}},$$

and $M = a\mu_e H_0\sqrt{\dfrac{\sigma}{\eta_0}}$ is the Hartman number.

Under lubrication approach, neglecting the terms of order δ and Re, we get

$$\mathrm{t}\frac{\partial p}{\partial x} = \frac{\partial}{\partial y}\left[1+\left(\frac{n-1}{2}\right)We^2\left(\frac{\partial u}{\partial y}\right)^2\right]\frac{\partial u}{\partial y}-M^2(u+1) \quad (2.13)$$

$$\frac{\partial p}{\partial y} = 0 \quad (2.14)$$

The corresponding boundary conditions in wave frame of reference are given by

$$u+\beta\left[\frac{\partial u}{\partial y}+\left(\frac{n-1}{2}\right)We^2\left(\frac{\partial u}{\partial y}\right)^3\right] = -1$$

$$\text{at } y=h=1+\phi\cos 2\pi x, \quad (2.15)$$

$$\frac{\partial u}{\partial y}=0 \text{ at } y=0. \quad (2.16)$$

Equations (2.13), (2.14) indicate that $p\neq p(y)$. Therefore Eq. (2.13) can be rewritten as

$$\frac{dp}{dx} = \frac{\partial}{\partial y}\left\{\left[1+\left(\frac{n-1}{2}\right)We^2\left(\frac{\partial u}{\partial y}\right)^2\right]\frac{\partial u}{\partial y}\right\},-M^2(u+1)$$
$$(2.17)$$

The volume flow rate q in a wave frame of reference is given by

$$q = \int_0^h u\,dy. \quad (2.18)$$

The instantaneous flux $Q(X,t)$ in the laboratory frame is

$$Q(x,t) = \int_0^h u\,dy = \int_0^h (u+1)dy = q+h. \quad (2.19)$$

The time average flux over one period $T\left(=\dfrac{\lambda}{c}\right)$ of the peristaltic wave is

$$\overline{Q} = \frac{1}{T}\int_0^T Q\,dt = \int_0^1 (q+h)dx = q+1. \quad (2.20)$$

3. Solution

For perturbation solution, we expand u, q and p as

$$u = u_0 + We^2 u_1 + O(We^4) \quad (3.1)$$

$$q = q_0 + We^2 q_1 + O(We^4) \quad (3.2)$$

$$p = p_0 + We^2 p_1 + O(We^4) \quad (3.3)$$

Substituting these equations in the Eq. (2.17) and in the boundary conditions (2.15) and (2.16), we get

(i) System of order We^0

$$\frac{dp_0}{dx} = \frac{\partial^2 u_0}{\partial y^2} - M^2(u_0+1). \quad (3.4)$$

The boundary conditions are

$$u_0 + \beta\frac{\partial u_0}{\partial y} = -1 \text{ at } y=h \quad (3.5)$$

$$\frac{\partial u_0}{\partial y} = 0 \text{ at } y=0 \quad (3.6)$$

(ii) System of order We^2

$$\frac{dp_1}{dx} = \frac{\partial^2 u_1}{\partial y^2} + \left(\frac{n-1}{2}\right)\frac{\partial}{\partial y}\left[\left(\frac{\partial u_0}{\partial y}\right)^3\right] - M^2 u_1 \quad (3.7)$$

The boundary conditions are

$$u_1 + \beta\left[\frac{\partial u_1}{\partial y}+\left(\frac{n-1}{2}\right)\left(\frac{\partial u_0}{\partial y}\right)^3\right] = -1 = 0 \text{ at } y=h \quad (3.8)$$

$$\frac{\partial u_1}{\partial y} = 0 \text{ at } y=0 \quad (3.9)$$

(iii) Solution for system of order We^0

Solving Eq. (3.4) and then using the boundary condition equations (3.5) and (3.6), we get

$$u_0 = \frac{1}{M^2}\frac{dp_0}{dx}\left(\frac{\cosh My}{A_1}-1\right)-1 \quad (3.10)$$

where $A_1 = \cosh Mh + \beta\sinh Mh$ and the volume flow rate q_0 is given by

$$q_0 = \int_0^h u_0\,dy = \frac{1}{M^3}\frac{dp_0}{dx}\left[\frac{\sinh Mh - MhA_1}{A_1}\right]-h \quad (3.11)$$

From Eq. (6.3.11), we get

$$\frac{dp_0}{dx} = \frac{A_1(q_0+h)M^3}{\sinh Mh - MhA_1}. \quad (3.12)$$

(iv) Solution for system of order We^2

Solving Eq. (3.7) using the Eq. (3.10) and the boundary conditions (3.8) and (3.9), we get

$$u_1 = \frac{1}{M^2}\frac{dp_1}{dx}\left[\frac{\cosh My}{A_1} - 1\right]$$

$$+ \frac{3(n-1)}{64M^4 A_1^3}\left(\frac{dp_0}{dx}\right)^3 \left[\begin{array}{c}\dfrac{A_5 \cosh My}{A_1} - \cosh 3My \\ + 4My\sinh My\end{array}\right] \quad (3.13)$$

where $A_2 = \cosh 3Mh - 4Mh\sinh Mh$,

$A_3 = 3M\sinh 3Mh - 4M\sinh Mh - 4M^2 h\cosh Mh$,

$A_4 = \dfrac{32}{3}M\sinh^3 Mh$ and $A_5 = A_2 + \beta A_3 - \beta A_4$.

and the volume flow rate q_1 is given by

$$q_1 = \int_0^h u_1 dy$$

$$= \frac{1}{A_1 M^3}\frac{dp_1}{dx}\left[\sinh Mh - MhA_1\right] + \frac{(n-1)A_6}{64M^5 A_1^4}\left(\frac{dp_0}{dx}\right)^3$$
$$(3.14)$$

where $A_6 = 3A_5\sinh Mh - A_1\sinh 3Mh$

$+ 12MhA_1\cosh Mh - 12A_1\sinh Mh$

From Eq. (3.14) and Eq. (3.12), we have

$$\frac{dp_1}{dx} = \frac{q_1 M^3 A_1}{(\sinh Mh - MhA_1)} - \frac{(n-1)A_6 M^7 (q_0 + h)^3}{64(\sinh Mh - MhA_1)^4}$$
$$(3.15)$$

Substituting from Equations (3.10) and (3.13) into the Eq. (3.1) and using the relation $\dfrac{dp_0}{dx} = \dfrac{dp}{dx} - We^2\dfrac{dp_1}{dx}$

and neglecting terms greater than $O(We^2)$, we get

$$\frac{dp}{dx} = \left(\frac{M^3 A_1 (q+h)}{(\sin Mh - MhA_1)}\right.$$

$$\left. - We^2 \frac{A_6 (n-1)M^7 (q+h)^3}{64(\sin Mh - MhA_1)^4}\right) \quad (3.16)$$

The dimensionless pressure rise per one wavelength in the wave frame is defined as

$$\Delta p = \int_0^1 \frac{dp}{dx}dx \quad (3.17)$$

4. Results and Discussions

Fig. 2 shows the variation of axial pressure gradient $\dfrac{dp}{dx}$ with We for $\phi = 0.6$, $M = 1, \beta = 0.1$ and $n = 0.4$. It is found that, the axial pressure gradient $\dfrac{dp}{dx}$ decreases with increasing We.

The variation of axial pressure gradient $\dfrac{dp}{dx}$ with n for $\phi = 0.6$, $M = 1$, $\beta = 0.1$ and $We = 0.1$ is shown in Fig. 3. It is observed that, the axial pressure gradient $\dfrac{dp}{dx}$ increases with increasing n.

Fig. 4 depicts the variation of axial pressure gradient $\dfrac{dp}{dx}$ with β for $\phi = 0.6$, $M = 1, We = 0.1$ and $n = 0.4$. It is found that, the axial pressure gradient $\dfrac{dp}{dx}$ decreases with an increase in β.

The variation of axial pressure gradient $\dfrac{dp}{dx}$ with M for $\phi = 0.6$, $We = 0.1, \beta = 0.1$ and $n = 0.4$ is depicted in Fig. 5. It is noted that, the axial pressure gradient $\dfrac{dp}{dx}$ increases with increasing M.

Fig. 6 illustrates the variation of axial pressure gradient $\dfrac{dp}{dx}$ with ϕ for $We = 0.1$, $M = 1, \beta = 0.1$ and $n = 0.4$. It is observed that, the axial pressure gradient $\dfrac{dp}{dx}$ increases with an increase in ϕ.

The variation of pressure rise Δp with time-averaged volume flow rate $\overline{Q}$ for different values of We with $\phi = 0.6$, $M = 1$, $\beta = 0.1$ and $n = 0.4$ is presented in Fig. 7. It is found that, the time-averaged volume flow rate $\overline{Q}$ decreases with increasing We in the pumping region, while it increases with increasing We in both the free pumping and co pumping regions.

Fig. 8 shows the variation of pressure rise Δp with time-averaged volume flow rate $\overline{Q}$ for different values of n with $\phi = 0.6$, $M = 1$, $\beta = 0.1$ and $We = 0.1$. It is observed that, the time-averaged volume flow rate $\overline{Q}$ increases with increasing n in the pumping region, while it decreases with increasing n in both the free pumping and co pumping regions. Further, it is observed that, the pumping is more for Newtonian fluid $(n \to 1)$ than that of Carreau fluid.

The variation of pressure rise Δp with time-averaged volume flow rate $\overline{Q}$ for different values of β with $\phi = 0.6$, $M = 1$, $We = 0.1$ and $n = 0.4$ is presented in

Fig. 9. It is found that, the time-averaged volume flow rate $\overline{Q}$ decreases with increasing β in both the pumping and free pumping regions, while it increases with increasing β in the co pumping region for chosen $\Delta p\left(<0\right)$.

Fig. 10 depicts the variation of pressure rise Δp with time-averaged volume flow rate $\overline{Q}$ for different values of M with $\phi = 0.6$, $n = 0.4$, $\beta = 0.1$ and $We = 0.1$. It is observed that, the time-averaged volume flow rate $\overline{Q}$ increases with increasing M in the pumping region, while it decreases with increasing M in both the free pumping and co pumping regions. The variation of pressure rise Δp with time-averaged volume flow rate $\overline{Q}$ for different values of ϕ with $n = 0.4$, $M = 1$, $\beta = 0.1$ and $We = 0.1$ is presented in Fig. 11. It is noted that, the time-averaged volume flow rate $\overline{Q}$ increases with increasing ϕ in both the pumping and free pumping regions, while it decreases with increasing ϕ in the co pumping region for chosen $\Delta p\left(<0\right)$.

5. Conclusion

In this chapter, we studied the influence of slip on the peristaltic flow of a carreau fluid in a planar channel with the effect of a magnetic field under the assumptions of long wavelength and low-Reynolds number assumptions. It is observed that, the axial pressure gradient and time averaged flux in the pumping region increases with increasing n, M and ϕ, whereas they decreases with increasing We and β.

References

[1] EI-Shehawey E.F., N.T., EI-Dabe and I.M.EI-Desoky, Slip effects on the Peristaltic flow of a Non-Newtonian Maxwellian Fluid, Acta Mech., 186 (2006), 141-159.
[2] El Misery, A. M., El Shehawey, E. F. and Hakeem, A. A. Peristaltic motion of an incompressible generalized Newtonian fluid in a planar channel, J. Phys. Soc. Jpn., 65 (1996), 3524-3529.
[3] El Shehawey, E.F., EL Misery, A. M., and Hakeem, A. A. Peristaltic motion of generalized Newtonian fluid in a non-uniform channel, J. Phys. Soc. Jpn., 67 (1998), 434-440.
[4] El-Dabe, N. T.M., Fouad, A. and Hussein, M.M. Magnetohydrodynamic flow and heat transfer for a peristaltic motion of Carreau fluid through a porous medium, Punjab University Journal of Mathematics, 42(2010), 1-16.
[5] Hayat, T., Mohammed, F. M. and Asghar .S. Peristaltic flow of magneto hydrodynamic Johnson-segalman fluid, Nonlinear Dynamics, 40 (2005), 375-385.
[6] Hayat, T., Wang, Y., Siddiqui, A.M., Hutter, K. and ASGHAR, S. Peristaltic transport of a third-order fluid in a circular cylindrical tube, Math. Models & Methods in Appl. Sci., 12(2002), 1691-1706.
[7] Hayat, T., Wang, Y., Siddiqui, A.M., and Hutter, K. Peristaltic motion of a Johnson – Segalman fluid in a planar channel, Math. Problems in Engng. 1 (2003), 1-23.
[8] Mekheimer Kh. S. Non linear peristaltic transport through a porous medium in an inclined planar channel, J. Porous Media, 6(2003), 190-202.
[9] Mekheimer, Kh.S. and Al-Arabi, T. H. Nonlinear peristaltic transport of MHD flow through a porous medium, Int. J. Math. Math. Sci., 26(2003), 1663-1682.
[10] Noreen, S., Hayat, T. and Alsaedi, A. Study of slip and induced magnetic field on the peristaltic flow of pseudoplastic fluid, International Journal of Physical Sciences, Vol. 6(36)(2011), 8018-8026.
[11] Shapiro, A.H., Jaffrin, M.Y and Weinberg, S.L. Peristaltic pumping with long wavelengths at low Reynolds number, J. Fluid Mech. 37(1969), 799-825.
[12] Siddiqui, A. M., Hayat, T. and Masood, K. Magnetic fluid induced by peristaltic waves, Journal of Physical Society of Japan, 73(2004), 2142-2147.
[13] Siddiqui, A.M. and Schwarz, W.H. Peristaltic flow of a second order fluid in tubes, J. Non-Newtonian Fluid Mech., 53(1994), 257-284.
[14] Srivastava, L. M., and Agrawal, R. P. Oscillating flow of a conducting fluid with a suspension of spherical particles, J. Appl. Mech. 47(1980), 196-199.
[15] Srivastava, L.M., and Srivastava, V.P. Peristaltic transport of a non – Newtonian fluid: application to the vas deferens and small intestine, Annals Biomed. Engng., 13(1985), 137-153.
[16] Stud, V.K., Sephon, G.S. and Mishra, R.K., Pumping action on flow by a magnetic field, Bull. Math. Biol. 39 (1977), 385-390.
[17] Subba Reddy, M.V., Jaya Rami Reddy, B., Sudhakar Reddy, M. and Uma Maheswar, S. Non-linear peristaltic flow of a fourth grade fluid through a porous medium in an inclined asymmetric channel, International Journal of Fluids Engineering, 3(2011), 381-395.
[18] Subba Reddy, M.V., Jayarami Reddy, B., Nagendra, N. and Swaroopa, B. Slip effects on the peristaltic motion of a Jeffrey fluid through a porous medium in an asymmetric channel under the effect magnetic field, Journal of Applied Mathematics and Fluid Mechanics, 4(2012), 59-72.
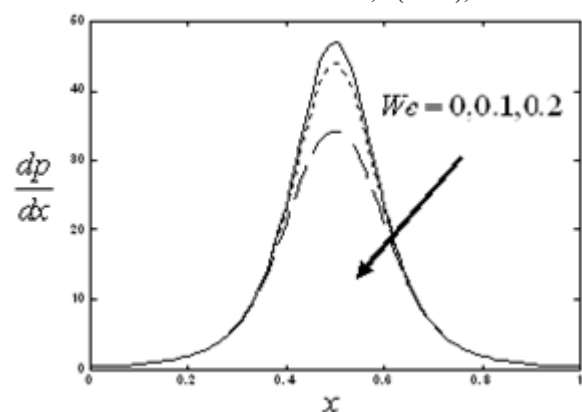
Figure 2: The variation of axial pressure gradient $\dfrac{dp}{dx}$ with We for $\phi = 0.6$, $M = 1$, $\beta = 0.1$ and $n = 0.4$.
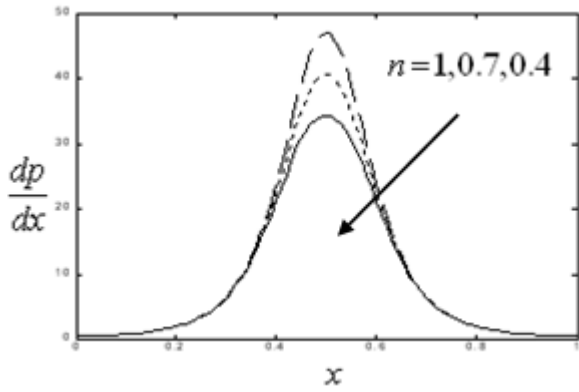
Paper ID: ART20171038

358

Figure 3: The variation of axial pressure gradient $\dfrac{dp}{dx}$ with n for $\phi = 0.6$, $M = 1$, $\beta = 0.1$ and $We = 0.1$.
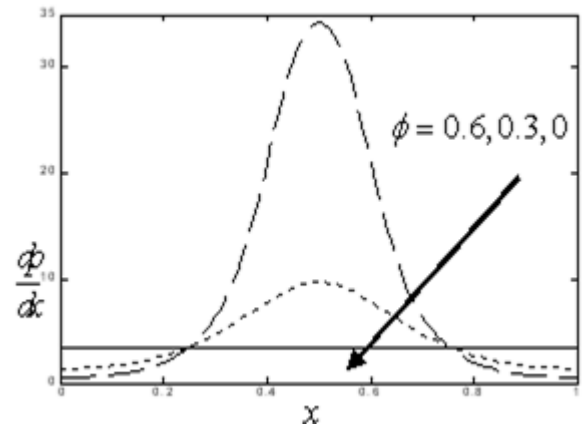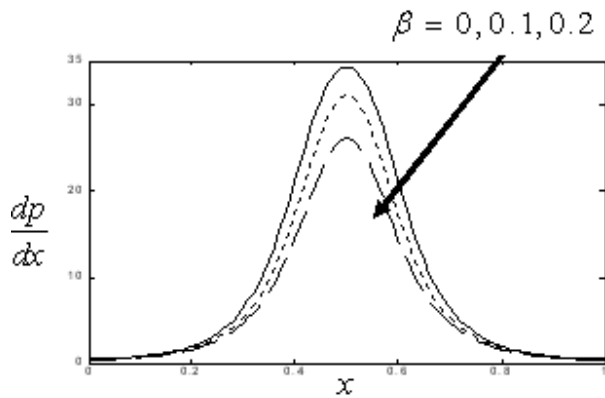

Figure 4: The variation of axial pressure gradient $\dfrac{dp}{dx}$ with β for $\phi = 0.6$, $M = 1$, $We = 0.1$ and $n = 0.4$.
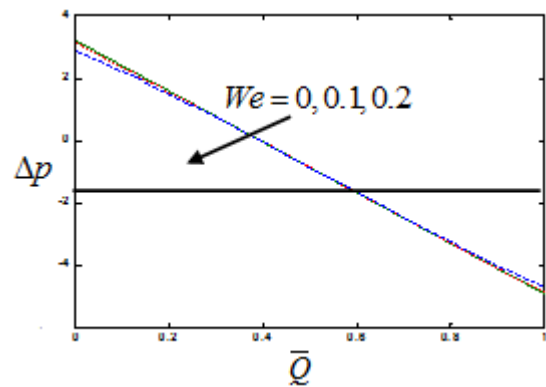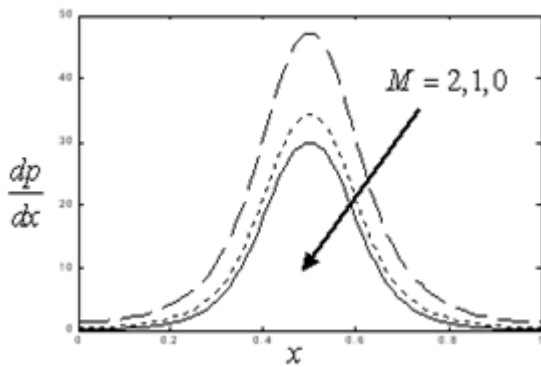

Figure 5: The variation of axial pressure gradient $\dfrac{dp}{dx}$ with M for $\phi = 0.6$, $We = 0.1$, $\beta = 0.1$ and $n = 0.4$.
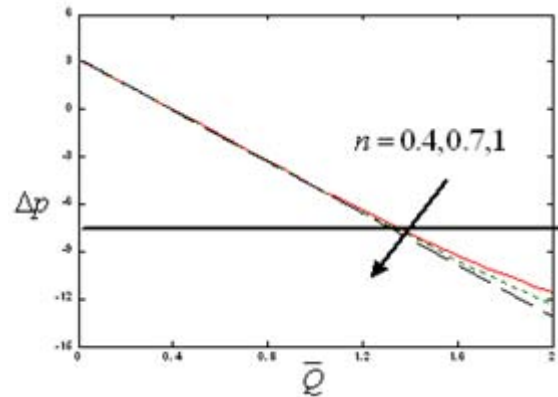

Figure 6: The variation of axial pressure gradient $\dfrac{dp}{dx}$ with ϕ for $We = 0.1$, $M = 1$, $\beta = 0.1$ and $n = 0.4$.

Figure 7: The variation of pressure rise Δp with time-averaged volume flow rate $\overline{Q}$ for different values of We with $\phi = 0.6$, $M = 1$, $\beta = 0.1$ and $n = 0.4$

Figure 8: The variation of pressure rise Δp with time-averaged volume flow rate $\overline{Q}$ for different values of n with $\phi = 0.6$, $M = 1$, $\beta = 0.1$ and $We = 0.1$.
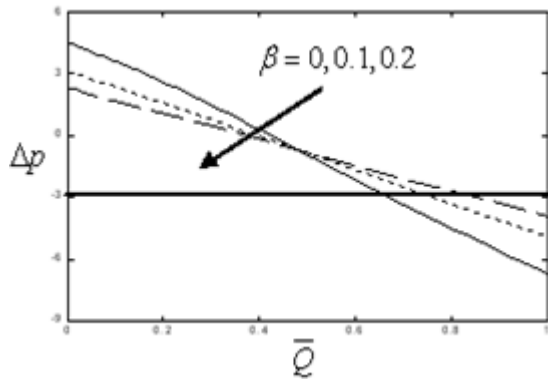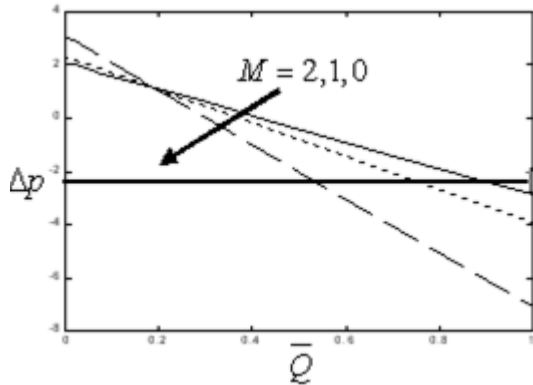
Paper ID: ART20171038

Figure 9: The variation of pressure rise Δp with time-averaged volume flow rate $\overline{Q}$ for different values of β with $\phi = 0.6$, $M = 1$, $We = 0.1$ and $n = 0.4$.

Figure 10: The variation of pressure rise Δp with time-averaged volume flow rate $\overline{Q}$ for different values of M with $\phi = 0.6$, $We = 0.1$, $\beta = 0.1$ and $n = 0.4$.
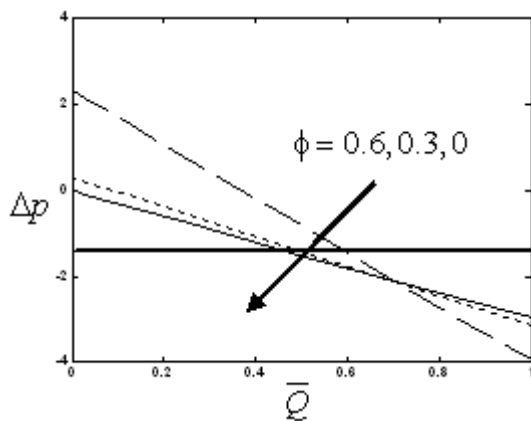

Figure 11: The variation of pressure rise Δp with time-averaged volume flow rate $\overline{Q}$ for different values of We with $\phi = 0.6$, $M = 1$, $\beta = 0.1$ and $n = 0.4$.